Velocity-free attitude reorientation of a flexible spacecraft with attitude constraints

Qiang Shen[1], Chengfei Yue[2], and Cher Hiang Goh[3]
National University of Singapore, 21 Lower Kent Ridge Rd, Singapore 119077

The velocity-free feedback control problem associated with rest-to-rest attitude reorientation for a flexible spacecraft in the presence of attitude-constrained zones is addressed. Attitude-constrained zones are parameterized as a convex set in terms of unit quaternion. Based on such a parameterization, a novel quadratic potential function is proposed with a global minimum at the desired attitude and high potential close to the forbidden zones. An velocity-free attitude controller is then developed by introducing an auxiliary quaternion dynamics to achieve asymptotic stability of the closed-loop system for flexible spacecraft in the absence of angular velocity measurements, meanwhile, avoiding forbidden attitudes that may harm on-board sensitive payloads or sensors. Application examples of the attitude control problem with consideration of attitude constraints are presented using the proposed method, and the results are demonstrated by simulation.

I. Introduction

ONE of the essential function for various spacecrafts is to point an on-board instrument's boresight along a prescribed inertial direction. In such a mission, instruments equipped on the spacecraft are sensitive payloads that are required to be kept sufficiently far away from unwanted celestial objects or bright source of energy. In view of this requirement, the capacity of attitude

---

[1] Associate Scientist, Temasek Laboratories, 5A Engineering Drive 1, Singapore 117508.
[2] PhD Student, Department of Electrical and Computer Engineering, 4 Engineering Drive 3, 117583 Singapore.
[3] Adjunct Professor, Department of Electrical and Computer Engineering, 4 Engineering Drive 3, 117583 Singapore.

controller to handle attitude constraints should be guaranteed. Otherwise, it will lead to damage of certain payloads and inferior control performance. For example, the infrared telescopes may be required to slew from one direction in space to another without direct exposure to the sun vector or other infrared bright regions [1]. Generally, this type of attitude maneuver can be regarded as a spacecraft reorientation problem in the presence of attitude-constrained zones and has attracted more and more attention in practical spacecraft missions.

A satellite's motion is governed by kinematic and dynamic equations, and the mathematical models are highly nonlinear and coupled. Extensive nonlinear control algorithms have been proposed for solving the spacecraft reorientation problem, such as proportional-derivative feedback control [2, 3], sliding mode control [4–6], backstepping control [7, 8], adaptive control [9], and inverse optimal control [10, 11]. However, it should be noted that attitude constraints are not taken into account in above mentioned literatures. On the other hand, attitude reorientation problem with consideration of attitude-constrained zones has been examined in only a few research works. Approaches to solve constrained attitude control problem can be generalized into two main categories: path planning methods and potential function methods. The path planning methods determine a feasible attitude trajectory before the reorientation maneuver according to the geometric relations with the exclusion zones. Consequently, a constraint-free attitude control law is implemented to follow the designed attitude path. In [12], based on the analysis of the vectorial kinematics on sphere, attitude motion planning was considered in the presence of bright objects and a communication link with ground station is maintained. In [13], assuming that there exists an constraint-free guidance loop, a randomized attitude slew planning algorithm was proposed to determine a time-parameterized sequence of "virtual attitude" that effectively steers the current attitude to the target attitude while avoiding constraints violations. In [14], the unit celestial sphere was discretized into a graph using an icosahedron-based pixelization subroutine, and the A^* pathfinding approach was employed to find an admissible minimum path-cost trajectory. In [15], a maneuver planning strategy was derived to accomplish the required single-axis pointing of an underactuated spacecraft in the presence of obstacles along the angular path and constraints on admissible rotation axes.

Although the path planning based methods are able to handle certain classes of attitude con-

straints, these methods have a disadvantage that they could not be extended to more complex scenarios, involving multiple celestial constrained zones, as often encountered in spacecraft missions [16]. Meanwhile, since path planning techniques are usually based on computationally demanding search methods, the computational tractability and closed-loop stability of the overall system may not be guaranteed using path planning based methods [17]. On contrary, potential function methods formulate the attitude constrained zones in the context of an artificial potential, which is further used for synthesizing the corresponding attitude control law to avoid unwanted celestial objects while achieving the desired attitude. Since this kind of approach is analytical without the need of any change in the overall structure of the attitude control software or hardware, it is suitable for on-board computation and provides flexible autonomous operations. In [18], Gaussian function was used as potential function to describe the dynamical environment in which the spacecraft exists, and control torques are then chosen such that satellite attitude converges to the desired final orientation without violating a list of user defined pointing constraints. Since Euler angles are used to represent attitude in [18], the proposed control algorithm may suffer from singularity. Instead of using Euler angles, the unit quaternion not only prevents singularity but also reduces expensive computational load created by the Euler angle expression [19]. In [20], a repulsive potential function was used for constrained slew maneuver, where the camera's CCD chip is prevented from exposing to the Sun directly. In [17], attractive and repulsive components of the potential function are designed in quaternion error vector space to guarantee target attitude convergence and constrained direction avoidance, respectively. In [16], a convex logarithmic barrier potential was formulated using the convex parameterization of attitude constrain sets in the unit quaternion space, and two attitude control laws based on backstepping technique were proposed for the constrained attitude control problem.

In this paper, based on potential function methods, a velocity-free control law that can achieve rest-to-rest three-axis attitude reorientation with autonomous avoidance of the undesired celestial objects is presented for a flexible spacecraft. The spacecraft orientation in the presence of constraints are formulated in terms of unit quaternion and is further parameterized to a convex set representation. Since the proposed quadratic potential function is proved to be strictly convex, it has the

capability to not only handle multiple attitude constrained zones but also guarantee convergence towards the desired attitude. Following this, an auxiliary unit-quaternion dynamical system introduced in [21] is employed to synthesize the velocity-free attitude controller that achieves asymptotic stability towards the desired attitude. The advantage of the proposed velocity-free control scheme is the feature of simple design and structure, which is of great interest for aerospace industry with real-time implementation when onboard computing power is limited. To the best of the authors' knowledge, the result presented in this paper is the first attempt in literature to accomplish attitude reorientation for flexible spacecraft without using explicit velocity feedback, while attitude constraints are also addressed.

The remainder of this paper is organized as follows. In Section II, unit-quaternion is introduced for attitude representation, and flexible spacecraft dynamics and modelling of attitude constrained zones are described. In Section III, a quadratic potential function is properly designed to parameterize the attitude constrained zones as a convex set, and then an velocity-free attitude control law is developed to guarantee that the closed loop system is asymptotically stable. The simulation results are given in Section IV, followed by conclusions in Section V.

II. Preliminaries

In this paper, the unit-quaternion representation is used to describe the orientation of a spacecraft. A quaternion is defined as $\boldsymbol{Q} = [q_1\ q_2\ q_3\ q_0]^T = [\boldsymbol{q}^T\ q_0]^T \in \mathbb{Q}$, where the vector part $\boldsymbol{q} \in \mathbb{R}^3$, the scalar part $q_0 \in \mathbb{R}$, and $\mathbb{Q}$ is the set of quaternion. The notation "$\otimes$" denotes the quaternion multiplication operator of two quaternion $\boldsymbol{Q}_i = [\boldsymbol{q}_i^T\ q_{i0}]^T \in \mathbb{Q}$ and $\boldsymbol{Q}_j = [\boldsymbol{q}_j^T\ q_{j0}]^T \in \mathbb{Q}$, which is defined as follows:

$$\boldsymbol{Q}_i \otimes \boldsymbol{Q}_j = \begin{bmatrix} q_{i0}\boldsymbol{q}_j + q_{j0}\boldsymbol{q}_i + \boldsymbol{S}(\boldsymbol{q}_i)\boldsymbol{q}_j \\ q_{i0}q_{j0} - \boldsymbol{q}_i^T\boldsymbol{q}_j \end{bmatrix}, \tag{1}$$

and has the quaternion $\boldsymbol{Q_I} = [0\ 0\ 0\ 1]^T$ as identity element. The matrix $\boldsymbol{S}(\boldsymbol{x}) \in \mathbb{R}^{3\times3}$ is a skew-symmetric matrix satisfying $\boldsymbol{S}(\boldsymbol{x})\boldsymbol{y} = \boldsymbol{x} \times \boldsymbol{y}$ for any vectors $\boldsymbol{x}, \boldsymbol{y} \in \mathbb{R}^3$, and $\times$ denotes vector cross product. The set of unit quaternion $\mathbb{Q}_u$ is a subset of quaternion $\mathbb{Q}$ such that

$$\mathbb{Q}_u = \{\boldsymbol{Q} = [\boldsymbol{q}^T\ q_0]^T \in \mathbb{R}^3 \times \mathbb{R} \mid \boldsymbol{q}^T\boldsymbol{q} + q_0^2 = 1\}, \tag{2}$$

where the vector part $\boldsymbol{q} = \hat{\boldsymbol{n}} \sin(\frac{\phi}{2})$, and the scalar part $q_0 = \cos(\frac{\phi}{2})$; $\hat{\boldsymbol{n}}$ and ϕ refer to the Euler axis and the rotation angle about the Euler axis. The unit-quaternion conjugate or inverse is defined as $\boldsymbol{Q}^* = [-\boldsymbol{q}^T \ q_0]^T$. The quaternion satisfies the following important properties [22]:

$$\boldsymbol{\alpha} \otimes (\boldsymbol{\beta} \pm \boldsymbol{\gamma}) = \boldsymbol{\alpha} \otimes \boldsymbol{\beta} \pm \boldsymbol{\alpha} \otimes \boldsymbol{\gamma} \tag{3}$$

$$(\boldsymbol{\alpha} \otimes \boldsymbol{b})^* = \boldsymbol{\beta}^* \otimes \boldsymbol{\alpha}^* \tag{4}$$

$$(\varrho\boldsymbol{\alpha}) \otimes \boldsymbol{b} = \boldsymbol{\alpha} \otimes (\varrho\boldsymbol{\beta}) = \varrho(\boldsymbol{\alpha} \otimes \boldsymbol{\beta}) \tag{5}$$

$$(\boldsymbol{\alpha} \otimes \boldsymbol{\beta}) \otimes \boldsymbol{\gamma} = \boldsymbol{\alpha} \otimes (\boldsymbol{\beta} \otimes \boldsymbol{\gamma}) \tag{6}$$

$$\boldsymbol{\alpha}^T(\boldsymbol{\beta} \otimes \boldsymbol{\gamma}) = \boldsymbol{\gamma}^T(\boldsymbol{\beta}^* \otimes \boldsymbol{\alpha}) = \boldsymbol{\beta}^T(\boldsymbol{\alpha} \otimes \boldsymbol{\gamma}^*), \tag{7}$$

where ϱ is a constant.

A. Kinematics equation

The spacecraft kinematics in terms of unit-quaternion can be given by

$$\dot{\boldsymbol{Q}} = \frac{1}{2}\boldsymbol{Q} \otimes \boldsymbol{\nu}(\boldsymbol{\omega}) = \frac{1}{2}\begin{bmatrix} \boldsymbol{S}(\boldsymbol{q}) + q_0\boldsymbol{I}_3 \\ -\boldsymbol{q}^T \end{bmatrix} \boldsymbol{\omega}, \tag{8}$$

where $\boldsymbol{Q} = [q_1 \ q_2 \ q_3 \ q_0]^T = [\boldsymbol{q}^T \ q_0]^T \in \mathbb{Q}_u$ denotes the unit-quaternion describing the attitude orientation of the body frame $\mathcal{B}$ with respect to inertial frame $\mathcal{I}$ and satisfies the constraint $\boldsymbol{q}^T\boldsymbol{q} + q_0^2 = 1$, $\boldsymbol{\omega} \in \mathbb{R}^3$ is the inertial angular velocity vector of the spacecraft with respect to an inertial frame $\mathcal{I}$ and expressed in the body frame $\mathcal{B}$, $\boldsymbol{\nu}$: $\mathbb{R}^3 \to \mathbb{R}^4$ is defined as the mapping $\boldsymbol{\nu}(\boldsymbol{\omega}) = [\boldsymbol{\omega}^T \ 0]^T$.

Let $\boldsymbol{Q}_d \in \mathbb{Q}_u$ denote the desired attitude. In this paper, the rest-to-rest attitude reorientation problem of rotating a rigid spacecraft from its current attitude $\boldsymbol{Q}$ to a desired attitude $\boldsymbol{Q}_d$ is considered. The unit-quaternion error $\boldsymbol{Q}_e \in \mathbb{Q}_u$ is defined as $\boldsymbol{Q}_e = \boldsymbol{Q}_d^* \otimes \boldsymbol{Q} = [\boldsymbol{q}_e^T \ q_{e0}]^T$, which describes the discrepancy between the actual unit-quaternion $\boldsymbol{Q}$ and the desired unit-quaternion $\boldsymbol{Q}_d$. The kinematics represented by unit-quaternion error is described as [23]

$$\dot{\boldsymbol{Q}}_e = \frac{1}{2}\boldsymbol{Q}_e \otimes \boldsymbol{\nu}(\boldsymbol{\omega}_e), \tag{9}$$

where $\boldsymbol{\omega}_e = \boldsymbol{\omega} - \boldsymbol{R}(\boldsymbol{Q}_e)^T\boldsymbol{\omega}_d$, $\boldsymbol{R}(\boldsymbol{Q}_e)$ is the unit-quaternion error $\boldsymbol{Q}_e$ related rotation matrix [24] defined as $\boldsymbol{R}(\boldsymbol{Q}_e) = (q_{e0}^2 - \boldsymbol{q}_e^T\boldsymbol{q}_e)\boldsymbol{I}_3 + 2\boldsymbol{q}_e\boldsymbol{q}_e^T - 2q_{e0}\boldsymbol{S}(\boldsymbol{q}_e)$, and $\boldsymbol{\omega}_d$ denotes the desired angular velocity.

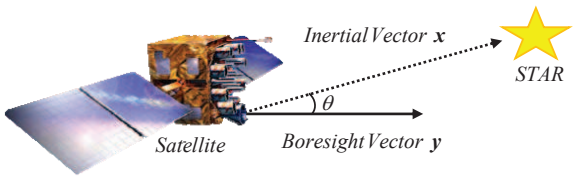

Fig. 1: Demonstration of attitude constraint.

In this paper, since rest-to-rest attitude reorientation problem is only considered, the desired angle velocity is $\boldsymbol{\omega}_d = 0$, which yields $\boldsymbol{\omega}_e = \boldsymbol{\omega}$. Therefore, the attitude error kinematics for rest-to-rest attitude reorientation maneuver in (9) can be rewritten as

$$\dot{\boldsymbol{Q}}_e = \frac{1}{2}\boldsymbol{Q}_e \otimes \boldsymbol{\nu}(\boldsymbol{\omega}) = \frac{1}{2}\begin{bmatrix} \boldsymbol{S}(\boldsymbol{q}_e) + q_{e0}\boldsymbol{I}_3 \\ -\boldsymbol{q}_e^T \end{bmatrix} \boldsymbol{\omega}. \tag{10}$$

B. Spacecraft Dynamics

The dynamics for the attitude motion of a spacecraft can be expressed by the following equations [9]:

$$\boldsymbol{J}\dot{\boldsymbol{\omega}} = -\boldsymbol{S}(\boldsymbol{\omega})\boldsymbol{J}\boldsymbol{\omega} + \boldsymbol{\tau} + \boldsymbol{d} \tag{11}$$

where $\boldsymbol{J} = \text{diag}\{J_1, J_2, J_3\} \in \mathbb{R}^{3\times3}$ denotes the positive definite inertia matrix of the spacecraft, $\boldsymbol{\tau} \in \mathbb{R}^3$ denotes the control torque about the body axes, $\boldsymbol{d} \in \mathbb{R}^3$ denotes the external disturbances.

To design the attitude controller, a sliding vector $\boldsymbol{s} = [s_1, s_2, s_3]^T \in \mathbb{R}^3$ is given by

$$\boldsymbol{s} = \boldsymbol{\omega} + k\boldsymbol{q}_e \tag{12}$$

Consequently, the attitude dynamics in terms of the sliding vector can be written as

$$\boldsymbol{J}\dot{\boldsymbol{s}} = \boldsymbol{f}(\boldsymbol{\omega}, \boldsymbol{Q}_e) + \boldsymbol{\tau} + \boldsymbol{d}, \tag{13}$$

where $\boldsymbol{f}(\boldsymbol{\omega}, \boldsymbol{Q}_e) = -\boldsymbol{S}(\boldsymbol{\omega})\boldsymbol{J}\boldsymbol{\omega} + \frac{k}{2}\left(\boldsymbol{S}(\boldsymbol{q}_e) + q_{e0}\boldsymbol{I}_3\right)\boldsymbol{\omega}$.

Assumption 1: The external disturbance $\boldsymbol{d}$ is bounded such that $\|\boldsymbol{d}\| \leq d_{\max}$, where $d_{\max}$ is a positive constant and $\|\cdot\|$ denotes the Euclidean norm.

C. Attitude Constraints Based on Unit-Quaternion

Suppose a half-cone angle strictly greater than θ should be maintained between the normalized boresight vector $\boldsymbol{y}$ of the spacecraft instrument and the normalized vector $\boldsymbol{x}$ pointing toward a certain celestial object, as shown in Fig. 1. This means that the cones with an apex angle of θ emanating from the sensitive on-board instruments should exclude the bright objects during the reorientation maneuver. When the attitude of the spacecraft is determined by $\boldsymbol{Q}$, the new boresight vector of the instrument in the inertial coordinates is

$$\begin{aligned}\boldsymbol{y}_I =&\boldsymbol{R}(\boldsymbol{Q})^T\boldsymbol{y}\\ =&(q_0^2-\boldsymbol{q}^T\boldsymbol{q})\boldsymbol{y}+2(\boldsymbol{q}^T\boldsymbol{y})\boldsymbol{q}+2q_0(\boldsymbol{q}\times\boldsymbol{y}),\end{aligned}\tag{14}$$

where $\boldsymbol{R}(\boldsymbol{Q})$ is a rotation matrix given by $\boldsymbol{R}(\boldsymbol{Q}) = (q_0^2-\boldsymbol{q}^T\boldsymbol{q})\boldsymbol{I}_3+2\boldsymbol{q}\boldsymbol{q}^T-2q_0\boldsymbol{S}(\boldsymbol{q})$. Then the constraints can be expressed by the vector dot product

$$\boldsymbol{x}\cdot\boldsymbol{y}_I<\cos(\theta),\tag{15}$$

Consequently, it follows from (15) that

$$q_0^2\boldsymbol{x}^T\boldsymbol{y}-\boldsymbol{q}^T\boldsymbol{q}\boldsymbol{x}^T\boldsymbol{y}+2(\boldsymbol{q}^T\boldsymbol{y})\boldsymbol{x}^T\boldsymbol{q}+2q_0\boldsymbol{q}^T(\boldsymbol{y}\times\boldsymbol{x})<\cos(\theta)\tag{16}$$

which can be further rewritten as

$$\boldsymbol{Q}^T\begin{bmatrix}\boldsymbol{x}\boldsymbol{y}^T+\boldsymbol{y}\boldsymbol{x}^T-(\boldsymbol{x}^T\boldsymbol{y})\boldsymbol{I}_3 & \boldsymbol{y}\times\boldsymbol{x}\\ (\boldsymbol{y}\times\boldsymbol{x})^T & \boldsymbol{x}^T\boldsymbol{y}\end{bmatrix}\boldsymbol{Q}<\cos(\theta).\tag{17}$$

Suppose there are i constrained objectives associated with the jth on-board sensitive instrument in the spacecraft rotational space. Then, the spacecraft attitude $\boldsymbol{Q}\in\mathbb{Q}_u$ for which the boresight vector $\boldsymbol{y}_j$ with respect to the ith celestial object should satisfy the following constraint

$$\boldsymbol{Q}^T\boldsymbol{M}_i^j\boldsymbol{Q}<\cos(\theta_i^j),\tag{18}$$

where

$$\boldsymbol{M}_i^j=\begin{bmatrix}A_i^j & b_i^j\\ b_i^{jT} & d_i^j\end{bmatrix}\tag{19}$$

with

$$A_i^j = \boldsymbol{x}_i \boldsymbol{y}_j^T + \boldsymbol{y}_j \boldsymbol{x}_i^T - (\boldsymbol{x}_i^T \boldsymbol{y}_j) \boldsymbol{I}_3,$$

$$b_i^j = \boldsymbol{y}_j \times \boldsymbol{x}_i, \quad d_i^j = \boldsymbol{x}_i^T \boldsymbol{y}_j,$$

$$i = 1, 2, \ldots, n, \quad j = 1, 2, \ldots, m. \tag{20}$$

Subsequently, to represent the possible attitude for the jth instrument and the ith celestial object, a subset $\mathbb{Q}_{p_i^j}$ of $\mathbb{Q}_u$ is specified as

$$\mathbb{Q}_{p_i^j} = \{\boldsymbol{Q} \in \mathbb{Q}_u \mid \boldsymbol{Q}^T \boldsymbol{M}_i^j \boldsymbol{Q} - \cos\theta_i^j < 0\}. \tag{21}$$

The angle θ_i^j is the constraint angle about the direction of the ith object specified by $\boldsymbol{x}_i$ for the jth instrument boresight vector $\boldsymbol{y}_j$. Without loss of generality, the domain of the angle θ_i^j for all i and j is restricted to be $(0, \pi)$. For $\boldsymbol{Q} \in \mathbb{Q}_{p_i^j}$, we have $\boldsymbol{Q}^T \boldsymbol{M}_i^j \boldsymbol{Q} - \cos\theta < 0$, which can be further written as $\boldsymbol{Q}^T \overline{\boldsymbol{M}}_i^j \boldsymbol{Q} < 0$ with $\overline{\boldsymbol{M}}_i^j = \boldsymbol{M}_i^j - \cos\theta_i^j \boldsymbol{I}_4$. For $\theta_i^j \in (0, \pi)$, one has

$$-2 < \lambda_{\min}(\overline{\boldsymbol{M}}_i^j) \leq \boldsymbol{Q}^T \overline{\boldsymbol{M}}_i^j \boldsymbol{Q} < \lambda_{\max}(\overline{\boldsymbol{M}}_i^j) < 2, \tag{22}$$

where $\lambda_{\min}(\overline{\boldsymbol{M}}_i^j)$ and $\lambda_{\max}(\overline{\boldsymbol{M}}_i^j)$ denote the minimal and maximal eigenvalue of matrix $\overline{\boldsymbol{M}}_i^j$, respectively. Then the set $\mathbb{Q}_{p_i^j}$ can be equivalently represented as a convex set

$$\widetilde{\mathbb{Q}}_{p_i^j} = \{\boldsymbol{Q} \in \mathbb{Q}_u \mid \boldsymbol{Q}^T \widetilde{\boldsymbol{M}}_i^j \boldsymbol{Q} < 2\}, \tag{23}$$

where $\widetilde{\boldsymbol{M}}_i^j$ is a positive-definite matrix. The proof of the boundedness of $\boldsymbol{Q}^T \overline{\boldsymbol{M}}_i^j \boldsymbol{Q}$ in (22) as well as its convex representation in (23) can be established by applying Proposition 3 and Proposition 4 in [16].

D. Angular Velocity Constraints

Due to the limited measurement range of the rate gyros or specific mission requirements, the constraints on angular velocity might be required. Suppose that the angular velocity information is available, the angular velocity constraints are given by

$$|\omega_1| \leq \omega_{1,\max}, \ |\omega_2| \leq \omega_{2,\max}, \ |\omega_3| \leq \omega_{3,\max} \tag{24}$$

where $\omega_{i,\max}$ $(i = 1, 2, 3)$ is the limitation of allowable operational angular velocities for each axis. $***$ statements that show its equivalence to rate constraints.

III. Velocity-Free Attitude Reorientation Controller Design

A. Potential Function Design

The potential function $V_a(\boldsymbol{Q})$: $\mathbb{Q}_p \to \mathbb{R}$, is defined as

$$V_a(\boldsymbol{Q}) = \sum_{j=1}^{m}\sum_{i=1}^{n} \frac{1}{\alpha(\boldsymbol{Q}^T \boldsymbol{M}_i^j \boldsymbol{Q} - \cos\theta_i^j)^2}, \tag{25}$$

where the set $\mathbb{Q}_p = \{\boldsymbol{Q} \in \mathbb{Q}_u \mid \boldsymbol{Q} \in \mathbb{Q}_{p_i^j}\}$ ($i = 1, 2, \ldots, n$, and $i = 1, 2, \ldots, m$) represents the possible attitudes of the spacecraft on which the boresight vector of the onboard instruments lie outside of the constrained attitude.

In addition, to satisfy the angular velocity constraints, a logarithmic potential function is proposed as

$$V_r(\boldsymbol{s}) = \frac{1}{2}\log\left[\frac{1}{\prod_{i=1}^{3} J_i(s_{i,\max}^2 - s_i^2)}\right], \tag{26}$$

where $s_{i,\max}$ is a positive constant defined as $s_{i,\max} = \omega_{i,\max} - k > 0$.

B. Adaptive Controller Design

The attitude regulation controller is designed as

$$\boldsymbol{\tau} = \boldsymbol{f}(\boldsymbol{\omega}, \boldsymbol{Q}_e) + \boldsymbol{\Upsilon}\left(-k_1\boldsymbol{s} + k_3 \mathrm{Vec}[\nabla V^* \otimes \boldsymbol{Q}]\right) - \hat{\bar{d}}\frac{\boldsymbol{\Upsilon}^{-1}\boldsymbol{s}}{\|\boldsymbol{\Upsilon}^{-1}\boldsymbol{s}\|} \tag{27}$$

with

$$\dot{\hat{\bar{d}}} = \rho\left[\|\boldsymbol{\Upsilon}^{-1}\boldsymbol{s}\| - \mu(\hat{\bar{d}} - \hat{d}_{max})\right] \tag{28}$$

$$\dot{\hat{d}}_{max} = \delta(\hat{\bar{d}} - \hat{d}_{max}), \tag{29}$$

where the operator Vec[$\cdot$] denotes the vector part of [$\cdot$], $\boldsymbol{\Upsilon} = \mathrm{diag}\{J_1(s_{1,\max}^2 - s_1^2), J_2(s_{2,\max}^2 - s_2^2), J_3(s_{3,\max}^2 - s_3^2)\}$, the variables k_1, k_2, k_3, ρ, μ, and δ are positive constants.

Consider the following Lyapunov candidate:

$$V_\ell = 2kk_1[\boldsymbol{q}_e^T\boldsymbol{q}_e + (1-q_0)^2] + 2k_3V_a(\boldsymbol{Q}) + V_r(\boldsymbol{s}) + \frac{1}{2\rho}(\hat{\bar{d}} - d_{\max})^2 + \frac{\mu}{2\delta}(\hat{d}_{\max} - d_{\max})^2. \tag{30}$$

The time derivative of V_ℓ is

$$\begin{aligned}\dot{V}_\ell =&2kk_1\boldsymbol{q}_e^T\boldsymbol{\omega} + 2k_3\nabla V_a^T(\frac{1}{2}\boldsymbol{Q}\otimes\boldsymbol{\nu}(\boldsymbol{\omega})) + \boldsymbol{s}^T\boldsymbol{\Upsilon}^{-1}\boldsymbol{J}\dot{s} + \frac{1}{\rho}(\hat{\bar{d}} - d_{\max})\dot{\hat{\bar{d}}} + \frac{\mu}{\delta}(\hat{d}_{\max} - d_{\max})\dot{\hat{d}}_{\max}\\ =&2kk_1\boldsymbol{\omega}^T\boldsymbol{q}_e - k_3\boldsymbol{\omega}^T\mathrm{Vec}[(\nabla V^*\otimes\boldsymbol{Q})] + \boldsymbol{s}^T\boldsymbol{\Upsilon}^{-1}\left[\boldsymbol{f}(\boldsymbol{\omega},\boldsymbol{Q}_e) + \boldsymbol{\tau} + \boldsymbol{d}\right]\\ &+ \frac{1}{\rho}(\hat{\bar{d}} - d_{\max})\dot{\hat{\bar{d}}} + \frac{\mu}{\delta}(\hat{d}_{\max} - d_{\max})\dot{\hat{d}}_{\max}\end{aligned} \tag{31}$$

Substituting the controller (27) and adaptive laws (28) and (29) in above equation, it yields

$$\begin{aligned}\dot{V}_\ell =&2kk_1\boldsymbol{\omega}^T\boldsymbol{q}_e - k_1\boldsymbol{s}^T\boldsymbol{s} - \hat{\bar{d}}\|\boldsymbol{\Upsilon}^{-1}\boldsymbol{s}\| + \boldsymbol{s}^T\boldsymbol{\Upsilon}^{-1}\boldsymbol{d}\\ &+ (\hat{\bar{d}} - d_{\max})\left[\|\boldsymbol{\Upsilon}^{-1}\boldsymbol{s}\| - \mu(\hat{\bar{d}} - \hat{d}_{max})\right] + \mu(\hat{d}_{\max} - d_{\max})(\hat{\bar{d}} - \hat{d}_{max})\\ \leq& - k_1k^2\boldsymbol{q}_e^T\boldsymbol{q}_e - k_1\boldsymbol{\omega}^T\boldsymbol{\omega} + \mu(\hat{\bar{d}} - \hat{d}_{max})(-\hat{\bar{d}} + d_{max} + \hat{d}_{\max} - d_{\max})\\ \leq& - k_1k^2\|\boldsymbol{q}_e\|^2 - k_1\|\boldsymbol{\omega}\|^2 - \mu(\hat{\bar{d}} - \hat{d}_{max})^2 \leq 0.\end{aligned} \tag{32}$$

Therefore, $\dot{V}_\ell$ is negative semi-definite, which implies that $\boldsymbol{q}_e$, $\boldsymbol{\omega}$, $V_a(\boldsymbol{Q})$, $V_r(\boldsymbol{s})$, $\hat{\bar{d}} - d_{\max}$, $\hat{d}_{\max} - d_{\max} \in L_\infty$. Since $d_{\max}$ is a constant, it is clear that $\hat{\bar{d}}$, $\hat{d}_{\max}\in L_\infty$. As a result, from (27), one can conclude that $\boldsymbol{\tau} \in L_\infty$. Upon integrating $\dot{V}_\ell$ from 0 to ∞, one obtains

$$V_\ell(0) - V_\ell(\infty) \geq k_1k^2\int_0^\infty \|\boldsymbol{q}_e(t)\|^2dt + k_1\int_0^\infty \|\boldsymbol{\omega}(t)\|^2dt + \mu\int_0^\infty (\hat{\bar{d}} - \hat{d}_{max})^2dt \tag{33}$$

Since the term on the left-hand side of the above inequality is bounded, it follows that $\boldsymbol{q}_e \in L_\infty \cap L_2$, $\boldsymbol{\omega} \in L_\infty \cap L_2$, and $\hat{\bar{d}} - \hat{d}_{max} \in L_\infty \cap L_2$. In addition, one can easily verify that $\dot{\boldsymbol{q}}_e \in L_\infty$, $\dot{\boldsymbol{\omega}} \in L_\infty$ and $\dot{\hat{\bar{d}}} - \dot{\hat{d}}_{max} \in L_\infty$ from (10), (11), (28), and (29). Consequently, by invoking Barbalat's lemma [27], it yields that

$$\lim_{t\to\infty}\boldsymbol{q}_e(t) = 0,\ \lim_{t\to\infty}\boldsymbol{\omega}(t) = 0,\ \lim_{t\to\infty}(\hat{\bar{d}}(t) - \hat{d}_{max}(t)) = 0 \tag{34}$$

In summary, we have the following theorem.

Theorem 1: The velocity-free controller (27), applied to the flexible spacecraft control systems expressed by (8), (11) and (**??**) in the presence of attitude constrained zones, guarantees that all closed-loop signals are bounded and that $\lim_{t\to\infty}\boldsymbol{\omega} = 0$ and $\lim_{t\to\infty}\boldsymbol{Q}(t) = \boldsymbol{Q}_d$.

IV. Simulation Results

To demonstrate the effectiveness and performance of the proposed controller, numerical simulation is performed to a flexible spacecraft in this section. It is assumed that the spacecraft carries a

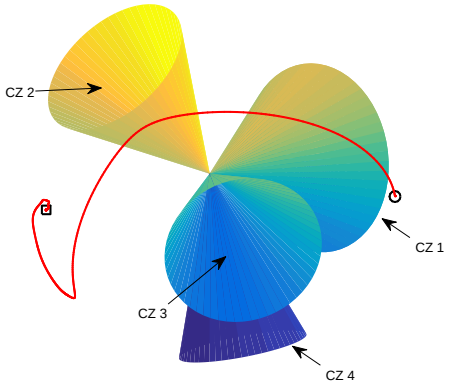

(a) Trajectory in three-dimension (3D); directions of initial and desired orientation are marked by “circle" and “square", respectively.

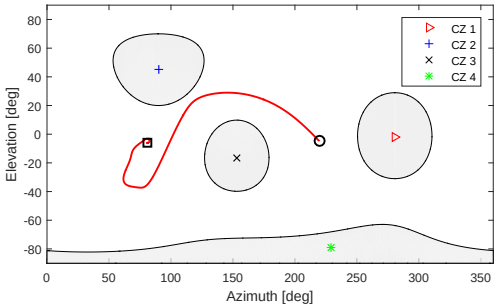

(b) Trajectory in two-dimensional (2D) cylindrical projection.

Fig. 2: Case I: Trajectory of sensitive instrument pointing direction in 3D and 2D under the proposed control law in (27).

light-sensitive instrument with a fixed boresight in the spacecraft body axes aligned with Z direction. The nominal main body inertia matrix of spacecraft is

$$\boldsymbol{J}_0 = \begin{bmatrix} 350 & 3 & 4 \\ 3 & 280 & 10 \\ 4 & 10 & 190 \end{bmatrix} \text{ kg} \cdot \text{m}^2 \tag{35}$$

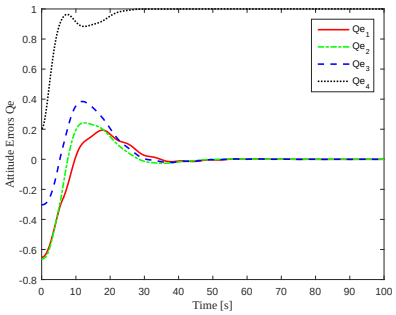

(a) Quaternion error $\boldsymbol{Q}_e$

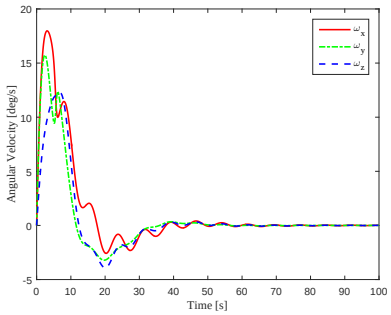

(b) Angular velocity $\boldsymbol{\omega}$

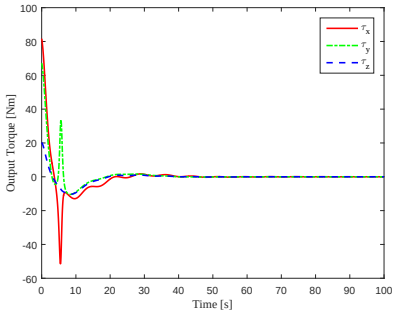

(c) Control torque $\boldsymbol{\tau}$

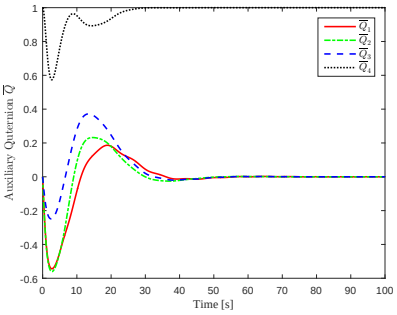

(d) Auxiliary quaternion $\bar{\boldsymbol{Q}}$

Fig. 3: Case I: Time responses of spacecraft attitude $\boldsymbol{Q}_e$, angular velocity $\boldsymbol{\omega}$, control torque $\boldsymbol{\tau}$, and auxiliary unit-quaternion $\bar{\boldsymbol{Q}}$ under the proposed control law in (27).

and the coupling matrix between the elastic and rigid dynamics is given by [9]

$$\delta = \begin{bmatrix} 6.45637 & 1.27814 & 2.15629 \\ -1.25619 & 0.91756 & -1.67264 \\ 1.11687 & 2.48901 & -0.83674 \\ 1.23637 & -2.6581 & -1.12503 \end{bmatrix} \sqrt{\text{kg}}\,\text{m/s}^2 \tag{36}$$

The natural frequencies are $\Lambda_1 = 0.7681$, $\Lambda_2 = 1.1038$, $\Lambda_3 = 1.8733$, $\Lambda_4 = 2.5496$ rad/s, and the corresponding damping ratios are $\zeta_1 = 0.05607$, $\zeta_2 = 0.08620$, $\zeta_3 = 0.1283$, $\zeta_4 = 0.2516$. In the simulation, the spacecraft is retargeting its sensitive instrument (such as infrared telescopes or interferometers) while avoiding four celestial objects (such as sun light or other bright objects) in the spacecraft reorientation configuration space. Four attitude-constrained zones are chosen without overlapping with each other. The details of the four attitude-constrained zones are given in Table 1, in which the normalized vectors pointing toward the corresponding celestial objects

are expressed with respect to the inertial frame. Both initial and desired attitude are chosen such that they are out of four attitude-constrained zones. The spacecraft is assumed to have the initial attitude $\boldsymbol{Q}(0) = [0.329\ 0.659\ -0.619\ -0.2726]^T$ and initial angular velocity $\boldsymbol{\omega}(0) = [0\ 0\ 0]^T$ rad/s. The controller gains in (27) are chosen as $k_1 = 0.3\boldsymbol{J}_p$, $k_2 = 0.05\boldsymbol{J}_p$, and $k_3 = 0.005\boldsymbol{J}_p$, where $\boldsymbol{J}_p = diag([350\ 280\ 190])$ is a diagonal matrix in which the nonzero values are identical to the diagonal values of $\boldsymbol{J}_0$. Note that each of the controller gains in simulation is selected as a multiplication of a constant and a diagonal matrix $\boldsymbol{J}_p$ containing diagonal elements of the inertia matrix. Although the control gains are not scale constants as defined in original controller (27), the overall stability can still be guaranteed. The benefit of the gain modification is that it is easier to select proper gains to get a satisfactory control performance. For the auxiliary unit-quaternion defined in (**??**), the variable $\boldsymbol{\Omega} = \boldsymbol{\Gamma}\tilde{\boldsymbol{q}}$ with $\boldsymbol{\Gamma} = [1.5\ 1.5\ 1.5]^T$. The variable α in potential function is chosen as $\alpha = 50$.

Since the initial and desired attitudes are randomly chosen outside of the attitude-constrained zones, two different cases should be considered in the simulation.

Table 1: Simulation parameters

Constrained Zone (CZ)	Constrained Object	Angle
CZ 1	[0.183 -0.983 -0.036]	30 deg
CZ 2	[0 0.707 0.707]	25 deg
CZ 3	[-0.853 0.436 -0.286]	25 deg
CZ 4	[0.122 -0.140 -0.983]	20 deg

A. Case I: The desired attitude is far away from attitude-constrained zones.

The desired attitude of the flexible spacecraft rotating to is selected as $\boldsymbol{Q}_d = [0.5\ -0.55\ -0.42\ -0.5207]^T$, which is far away from four attitude-constrained zones. More specifically, the target attitude is in a position at 51.64 deg from the center of the nearest attitude-constrained zone (i.e., CZ 2), which corresponds that the minimal angle between desired orientation and the boundary of the nearest forbidden cone is 26.64 deg. Fig. 2a shows the trajectory of sensitive instrument pointing

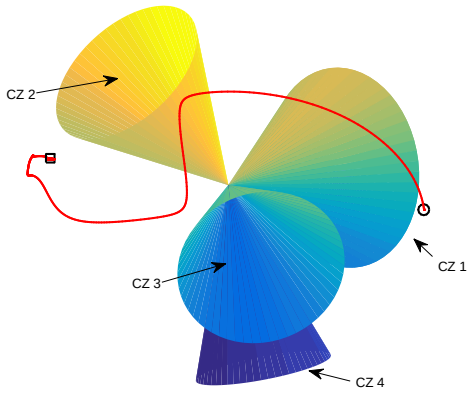

(a) Trajectory of sensitive instrument pointing direction in three-dimension (3D).

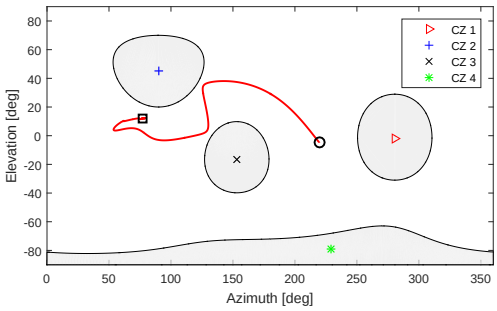

(b) Trajectory in two-dimensional (2D) cylindrical projection.

Fig. 4: Case II: Trajectory of sensitive instrument pointing direction in 3D and 2D under the proposed control law in (27).

direction in 3D during the rest-to-rest attitude maneuver, in which four attitude-constrained zones in Table 1 are plotted inside a celestial sphere. As shown Fig. 2a, the reorientation trajectory generated by the proposed controller in (27) avoids all four constrained zones while achieving the desired attitude. Fig. 3a depicts the same trajectories on the cylindrical projection of the corresponding celestial spheres. Fig. 3 describes details of the control performance in Case I, where the time histories for attitude error, angular velocity, control torque, and auxiliary quaternion are illustrated. It can be observed that the velocity-free controller in (27) obtains a satisfactory performance in the spacecraft rest-to-rest reorientation despite four attitude-constrained zones. From Figs. 3a and 3b, angular velocity has a longer stabilization time than that taking for attitude stabilization, and it

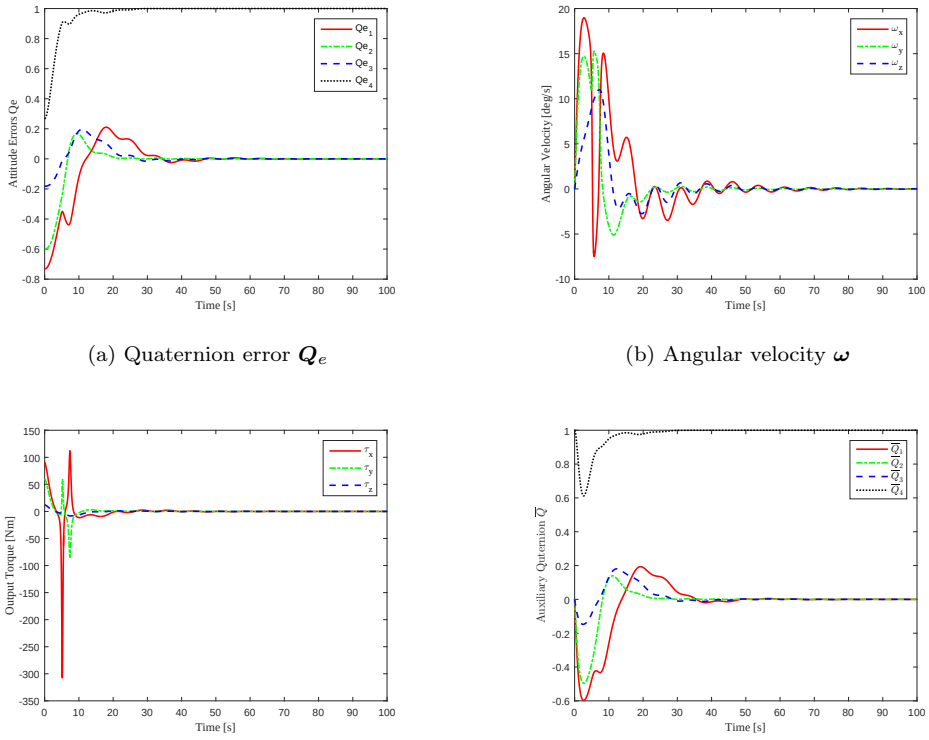

(a) Quaternion error $\boldsymbol{Q}_e$

(b) Angular velocity $\boldsymbol{\omega}$

(c) Control torque $\boldsymbol{\tau}$

(d) Auxiliary quaternion $\bar{\boldsymbol{Q}}$

Fig. 5: Case II: Time responses of spacecraft attitude $\boldsymbol{Q}_e$, angular velocity $\boldsymbol{\omega}$, control torque $\boldsymbol{\tau}$, and auxiliary unit-quaternion $\bar{\boldsymbol{Q}}$ under the proposed control law in (27).

experiences a short phase of oscillation but stabilizes to its steady state in 70 seconds. This is due to the fact that angular velocity is assumed to be unavailable in feedback control loop. As a result, the sensitive instrument' reorientation trajectory generated by the velocity-free controller may approach but not stay on the desired orientation firstly, and it eventually reaches the desired orientation until the angular velocity is stabilized. This phenomenon is consistent with results observed in Fig. 2.

B. Case II: The desired attitude is near to one of attitude-constrained zones

In this case, the desired attitude that the flexible spacecraft rotating to is $\boldsymbol{Q}_d = [0.38 \ -0.5 \ -0.5 \ -0.5963]^T$, which is quite near to the second attitude-constrained zone. the target attitude is in a position at 34.58 deg from the center of the nearest attitude-constrained zone (i.e., CZ 2), which corresponds that the minimal angle between desired orientation and the boundary of the nearest forbidden cone is 9.58 deg. As shown in Fig. 4, the pointing direction of the instrument

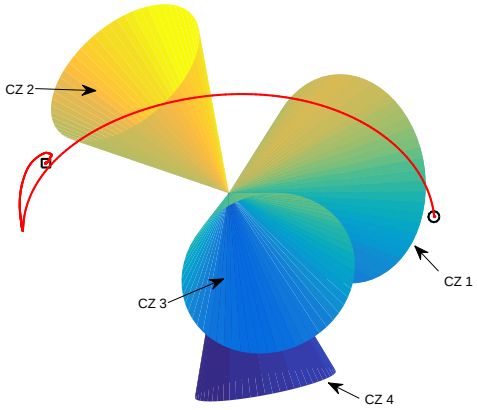

(a) Trajectory of sensitive instrument pointing direction in three-dimension (3D).

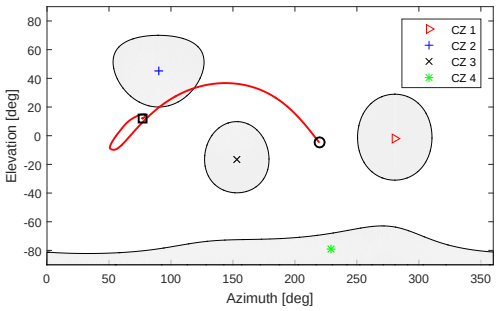

(b) Trajectory in two-dimensional (2D) cylindrical projection.

Fig. 6: Case II: Trajectory of sensitive instrument pointing direction in 3D and 2D using controller in [21].

generated by the proposed controller tries to reach the desired pointing direction from the initial pointing direction, but the second attitude-constrained cone lies on its way and prevents from passing directly. In order to keep out of this attitude-constrained cone, a large control toque in the opposite direction is produced which keeps the pointing direction away from the forbidden cone. Similar to the previous situation, the proposed controller generates a proper control action such that the third attitude-constrained cone is avoided, and finally drives the instrument to reach the desired pointing direction. The corresponding simulation results for the quaternion error, angular velocity, control torque, and auxiliary quaternion are shown in Fig. 5, from which it is clear that acceptable control performance is achieved despite the transient performance is not as good as that in Case I.

In addition, two sharp increases of the control torque are observed in Fig. 5c because a large control torque is required to keep out of the attitude-constrained zones. A comparison with the technique discussed in [21] is also considered, where velocity-free controller is developed without coping with attitude constraints. Fig. 6 reports the simulation results using controller in [21]. it is clear that the pointing trajectory goes into the second attitude-constrained cone, which may cause damage to the sensitive onboard instrument.

V. Conclusion

This paper focuses on the development of velocity-free attitude control laws for rest-to-rest maneuver of flexible spacecraft under attitude constraints. The constrained spacecraft orientations are parameterized as a convex set utilizing an intrinsic property of the attitude representation via unit quaternion. A new quadratic potential function is proposed to avoid the unwanted celestial objects by placing a large potential around the constrained directions. Based on such a potential function, a velocity-free attitude control law is developed to ensure the asymptotic stability of the closed loop system by using an auxiliary unit-quaternion dynamics. The performance of the proposed constrained attitude control algorithm has been discussed through numerical studies.

References

[1] McInnes, C. R., "Large Angle Slew Maneuvers with Autonomous Sun Vector Avoidance," *Journal of Guidance, Control, and Dynamics*, Vol. 17, No. 4, 1994, pp. 875-877. doi: 10.2514/3.21283

[2] Wie, B. and Barba, P. M., "Quaternion Feedback for Spacecraft Large Angle Maneuvers", *Journal of Guidance, Control, and Dynamics*, Vol. 8, No. 3, 1985, pp. 360-365. doi: 10.2514/3.19988

[3] Wen, J. T. Y. and Kreutz-Delgado, K., "The Attitude Control Problem", *IEEE Transactions on Automatic Control*, Vol. 36, No. 10, 1991, pp. 1148-1162. doi: 10.1109/9.90228

[4] Boskovic, J. D., Li, S. M., and Mehra, R. K., "Robust Adaptive Variable Structure Control of Spacecraft Under Control Input Saturation", *Journal of Guidance, Control, and Dynamics*, Vol. 24, No. 1, 2001, pp. 14-22. doi: 10.2514/2.4704

[5] Shen, Q., Wang, D. W., Zhu, S. Q., and Poh, E. K., "Integral-Type Sliding Mode Fault-Tolerant Control for Attitude Stabilization of Spacecraft", *IEEE Transactions on Control Systems Technology*, Vol. 23, No. 3, 2015, pp. 1131-1138. doi: 10.1109/TCST.2014.2354260

[6] Shen, Q., Wang, D. W., Zhu, S. Q., and Poh, E. K., "Finite-Time Fault-Tolerant Attitude Stabilization with Actuator Saturation", *IEEE Transactions on Aerospace and Electronic Systems*, Vol. 51, No. 3, 2015, pp. 2390-2405. doi: 10.1109/TAES.2015.130725

[7] Kim, K., and Kim, Y., "Robust Backstepping Control for Slew Maneuver Using Nonlinear Tracking Fucntion", *IEEE Transactions on Control Systems Technology*, Vol. 11, No. 6, 2003, pp. 822-829. doi: 10.1109/TCST.2003.815608

[8] Kristiansen, R., Nicklasson, P. J., and Gravdahl, J. T., "Satellite Attitude Control by Quaternion-Based Backstepping", *IEEE Transactions on Control Systems Technology*, Vol. 17, No. 1, 2009, pp. 227-232. doi: 10.1109/TCST.2008.924576

[9] Di Gennaro, S., "Output Stabilization of Flexible Spacecraft with Active Vibration Suppression", *IEEE Transactions on Aerospace and Electronic Systems*, Vol. 39, No. 3, 2003, pp. 747-759. doi: 10.1109/TAES.2003.1238733

[10] Krstic, M., and Tsiotras, P., "Inverse Optimal Stabilization of a Rigid Spacecraft", *IEEE Transactions on Automatic Control*, Vol. 44, No. 5, 1999, pp. 1042-1049. doi: 10.1109/9.763225

[11] Xin, M., and Pan, H., "Indirect Robust Control of Spacecraft Via Optimal Control Solution", *IEEE Transactions on Aerospace and Electronic Systems*, Vol. 48, No. 2, 2012, pp. 1798-1809. doi: 10.1109/TAES.2012.6178102

[12] Hablani, H. B., "Attitude Commands Avoiding Bright Objects and Maintaining Communication with Groud Station", *Journal of Guidance, Control, and Dynamics*, Vol. 22, No. 6, 1999, pp. 759-767. doi: 10.2514/2.4469

[13] Frazzoli, E., Dahleh, M. A., Feron, E., and Kornfeld, R. P., "A Randomized Attitude Slew Planning Algorithm for Autonomous Spacecraft," *AIAA Guidance, Navigation, and Control Conference and Exhibit*, AIAA, Montreal, Canada, 2001, pp. 1-8. doi: 10.2514/6.2001-4155

[14] Kjellberg, H. C., and Lightsey, E. G., "Discretized Constrained Attitude Pathfinding and Control for Satellites", *Journal of Guidance, Control, and Dynamics*, Vol. 36, No. 5, 2013, pp. 1301-1309. doi: 10.2514/1.60189

[15] de Angelis, E. L., Giulietti, F., and Avanzini, G., "Single-Axis Pointing of Underactuated Spacecraft in the Presence of Path Constraints", *Journal of Guidance, Control, and Dynamics*, Vol. 38, No. 1, 2015, pp. 143-147. doi: 10.2514/1.G000121

[16] Lee, U., and Mesbahi, M., "Feedback Control for Spacecraft Reorientation under Attitude Constraints Via Convex Potentials", *IEEE Transactions on Aerospace and Electronic Systems*, Vol. 50, No. 4, 2014, pp. 2578-2592. doi: 10.1109/TAES.2014.120240

[17] Avanzini, G.,Radice, G., and Ali, I., "Potential Approach for Constrained Autonomous Manoeuvres of a Spacecraft Equipped with a Cluster of Control Moment Gyroscopes", *Proceedings of the Institution of Mechanical Engineers, Part G: Journal of Aerospace Engineering*, Vol. 223, No. 3, 2009, pp. 285-296. doi: 10.1243/09544100JAERO375

[18] McInnes, C. R., "Non-Linear Control for Large Angle Attitude Slew Maneuver," *The Third ESA Symposium on Spacecraft Guidance, Navigation, and Control*, ESTEC, Noordwijk, the Netherlands, 1996, pp. 543-548. doi: 1997ESASP.381..543M

[19] Hamilton,W. R., "On Quaternions; or on a New System of Imaginaries in Algebra," *Philosophical Magazine*, Series 3, Vol. 25, No. 163, 1844, pp. 10-13. doi: 10.1080/14786444408644923

[20] Rafal, W., and Piotr, K., "Slew Maneuver Control for Spacecraft Equipped with Star Camera and Reaction Wheels," *Control Engineering Practice*, Vol. 13, No. 3, 2005, pp. 349-356. doi: 10.1016/j.conengprac.2003.12.006

[21] Tayebi, A., "Unit Quaternion-Based Output Feedback for the Attitude Tracking Problem", *IEEE Transactions on Automatic Control*, Vol. 53, No. 6, 2008, pp. 1516-1520. doi: 10.1109/TAC.2008.927789

[22] Chou, J. K. C., "Quaternion Kinematic and Dynamic Differential Equations", *IEEE Transactions on Robotics and Automation*, Vol. 8, No. 1, 1992, pp. 53-64. doi: 10.1109/70.127239

[23] Shuster, M. D., "A Survey of Attitude Representation", *Journal of the Astronautical Sciences*, Vol. 41, No. 4, 1993, pp. 439-517. doi: 1993JAnSc..41..439S

[24] Sidi, M. J., "Spacecraft Dynamics and Control", Cambridge Univ. Press, Cambridge, England, U.K., 1997.

[25] Ben-Tal, A., El Ghaoui, L., and Nemirovksi, A., "Robust Optimization", Princeton Univ. Press, 2009.

[26] Xiao, B., Hu, Q. L., and Zhang, Y. M., "Fault-Tolerant Attitude Control for Flexible Spacecraft without Angular Velocity Magnitude Measurement", *Journal of Guidance, Control, and Dynamics*, Vol. 34, No. 5, 2011, pp. 1556-1561. doi: 10.2514/1.51148

[27] Khalil, H. K., "Nonlinear Systms", Prentice-Hall, Upper Saddle, River, NJ, 2002